Dynamic Luminescence of Lead-Doped Calcium Zinc Germanate Clinopyroxene for Multimode Anti-Counterfeiting

Zishen Yang, Levi Spencer, Huixin Zhang, Zachary Burmood, Anjaneyulu Putta, Chaoyang Jiang

Department of Chemistry, University of South Dakota, Vermillion, SD 57069, USA

Abstract. Anti-counterfeiting plays an essential role in authenticating genuine documents and combating forged products. To further advance the anti-counterfeiting technology, there is a strong demand to design new functional materials with unique properties that will be appropriate for making multimode complex security labels. Recently, dynamic security labels have emerged as a new type of advanced anti-counterfeiting method as they can hold a much higher security level than those traditional static ones. In this paper, we reported that calcium zinc germanate (CZGO) clinopyroxenes doped with lead ions have several interesting optical properties, such as dynamic fluorescence, long persistent luminescence (PersL), and photochromism. We found that the concentration of lead dopants can significantly impact the reaction kinetics, as well as the crystallinity and luminescence properties of CZGO phosphors. By fully utilizing these unique properties, we have successfully fabricated several security labels with multi-level information encoding and dynamic optical performance. The combination of multimode and dynamic luminescence makes these labels extremely challenging to be illegally duplicated. With further optimization, these lead-doped CZGO clinopyroxene can be well-integrated into modern anti-counterfeiting techniques that will generate highly secure anti-counterfeiting labels to combat fake products.

Keywords: Dynamic luminescence; Solid-state synthesis; Persistent luminescence; Photochromism; Calcium zinc germanate; Anti-counterfeiting

Introduction

With the development and advances in the global economy, counterfeit activities have emerged as a significant challenge. Counterfeiting causes economic loss and poses risks to public health and homeland security. Various anti-counterfeiting approaches have been designed to battle counterfeiting activities. Single-layered approaches such as holograms,[1] watermark,[2] bar codes,[3, 4] and QR codes[5] have been well-established and applied in anti-counterfeiting. However, these single-layered approaches lack sufficient complexity, can be easily replicated, and are prone to reverse engineering by counterfeiters. Thus, researchers are designing more unique and complicated materials to enhance security. As a result, multilayered approaches such as security printing, surface-enhanced Raman spectroscopy (SERS),[6, 7] and RFID tags[8] have raised significant attention to combat counterfeiting. However, these multilayered approaches are usually static. It is necessary to aim for a dynamic anti-counterfeit approach with enhanced complexity and security.

In recent years, dynamic anti-counterfeiting techniques have been reported, which are associated with various working mechanisms, including dynamic upconversion luminescence,[9] persistent luminescence (PersL) /phosphorescence,[10-14] fluorescence,[15-17] and photochromism.[17, 18] Notably, organic materials like spiropyran and its derivatives have demonstrated excellent dynamic fluorescence properties due to their reversible structural changes.[15, 18-21] For instance, Yang et al. demonstrated the application of a spiropyran-loaded lanthanide metal-organic framework (SP@Ln-MOF).[15] The SP@Ln-MOF showed a reversible dynamic fluorescence color change from yellowish-green to orange to red within 60 seconds, which is excellent for anti-counterfeiting applications. In addition to organic phosphors, certain inorganic materials have also been explored as functional materials for dynamic anti-counterfeiting. Katumo *et al.* reported dynamic anti-counterfeiting applications using Gd_2O_2S: Eu^{3+}/Ti^{4+} phosphors.[14] In their work, changing the dopant concentration allowed the phosphor materials to have

persistent luminescence with different lifetimes. The authors then combine three different phosphors to form a series of digital numbers and utilize a cell phone to capture the persistent luminescence. The results showed a dynamic change of numbers, which could be used for dynamic anti-counterfeiting. Inorganic materials possess several advantages over organic counterparts, such as increased chemical inertness, excellent thermal/photostability, and enhanced durability in real-world applications. However, most inorganic materials used in dynamic anti-counterfeiting rely on upconversion or persistent luminescence; there is currently little research utilizing dynamic fluorescence inorganic materials.

Germanate materials have gained significant attention in the field of luminescence due to their excellent chemical stability. Numerous studies have focused on utilizing germanate as a host material that contains various dopants to create phosphor materials with exceptional luminescent properties. For example, germanate material Zn_2GeO_4 (ZGO) has been intensively studied in the last few decades[22-30], and ZGO-based phosphor materials have been utilized in anti-counterfeiting labels with excellent outcomes.[30-32] Other germanate materials could also be good candidates for anti-counterfeiting applications. One such material is $CaZnGe_2O_6$ (CZGO), which is a clinopyroxene material utilized in long persistent luminescence phosphors.[33-36] The dopants used in CZGO clinopyroxene include chromium (Cr);[35, 37] manganese (Mn);[33, 38] bismuth (Bi);[33, 39] dysprosium (Dy);[36] terbium (Tb),[34] and lead (Pb).[17] In particular, Dong et al. recently reported the synthesis and application of lead-doped CZGO (CZGO: Pb) with dynamic fluorescence and photochromic properties.[17] They found that CZGO with 1.4% Pb dopant can be integrated into PDMS films for advanced anti-counterfeiting applications. However, systematic investigation of the CZGO materials is still missing in the literature, such as the dopant concentration impact, reaction condition optimization, and luminescence mechanism study. It is essential to solve these obstacles to fully utilize these novel CZGO clinopyroxene for the application of advanced anti-counterfeiting.

In this work, we synthesized a series of lead-doped CZGO phosphors ($CaZnGe_2O_6$: Pb) with dopant concentrations ranging from 0.1% to 10% via a known solid-state synthetic method. CZGO phosphors were characterized with X-ray diffraction for the optimization of synthesis parameters such as reaction time and temperature.

The optical properties of CZGO, including dynamic fluorescence, photochromism, and persistent luminescence, were examined using optical imaging, spectroscopy, and time-dependent intensity measurements. Furthermore, we demonstrated that these lead-doped CZGO phosphors can be used in making multimode anti-counterfeiting labels with dynamic luminescent performance.

Experimental

Chemicals and Materials

$CaCO_3$ (Certified ACS) was purchased from Fisher Scientific, and ZnO (nanopowder) and GeO_2 (99.999%) were purchased from Millipore Sigma. PbO (99.7%) was purchased from BAKER ANALYZED™ Reagent. Commercially available acrylic gel was used as a medium for anti-counterfeiting paint. All chemicals and materials were used without further purification.

Synthesis and materials process

$CaCO_3$, ZnO, GeO_2, and PbO were weighed stoichiometrically, then mixed and ground using an agate mortar and pestle. The mixture was transferred into a 1.7 mL porcelain crucible and heated in a muffle furnace (Thermolyne 46900) at 1050 °C for a desired period of time. After the reaction, the products were cooled in the oven before being ground into a fine powder. For analysis, the phosphor materials were pressed into pellets using a Carver Manual pellet press. Anti-counterfeiting paint was produced by mixing phosphor powder with an acrylic gel/ water mixture.

Characterization

All phosphor samples were examined with powder X-ray diffraction (Rigaku Ultima IV). The fluorescence spectra and dynamic fluorescence spectrums were acquired with a Horiba Duetta Fluorescence and Absorbance Spectrometer. The UV excitation source is a portable UV lamp (ENF-240C, Spectroline), and the optical images were captured using an iPhone 12. Agilent Cary 5000 UV-Vis-NIR Spectrophotometer was used to measure the reflectance spectra of the compressed pellets. During the measure of dynamic fluorescence, each spectrum was acquired in 0.45 seconds, and the spectra were recorded every 0.5 seconds.

Results and discussion

The synthesized phosphor material, CZGO: 0.25% Pb, appears as an off-white powder in ambient conditions, as shown in Figure 1a. The phosphor emits a vibrant green fluorescence emission upon exposure to 254 nm UV irradiation, as seen in Figure 1b. Notably, this fluorescence undergoes a rapid transition to blue under one minute of continuous UV light exposure, as illustrated in Figure 1c. This phenomenon becomes particularly apparent when we use a spatula to remove the surface layer of the phosphor material, as shown in Figure S1. Immediately upon removal of the surface layer, we can easily observe the original green fluorescence from the freshly exposed phosphor materials (See Supporting Video). Subsequently, the green-emitting region transitions to blue and displays a fluorescence similar to the neighboring areas, which have been exposed to UV light continuously. Furthermore, upon discontinuing the UV irradiation, we observe a red-colored persistent luminescence (PersL), as depicted in Figure 1d. This PersL is notably strong and remains easily discernible to the naked eye, even 30 seconds after the cessation of the UV lamp.

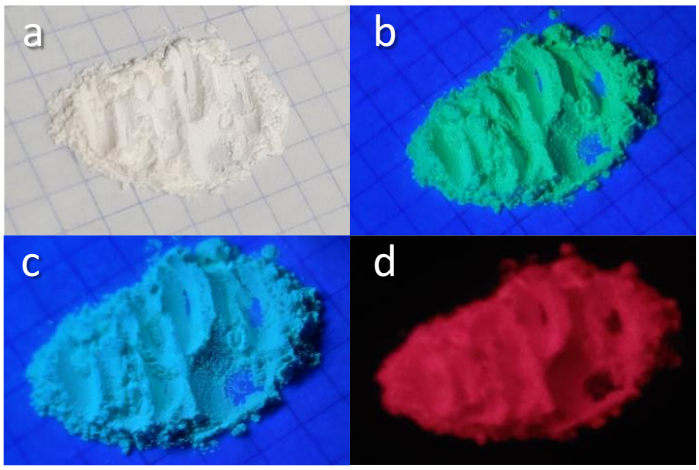

Figure 1. Photos of CZGO: Pb phosphor powder (a) under room light, (b) immediately under UV light, (c) one minute under UV light, and (d) after turning off the UV light.

The powder XRD pattern of the phosphor is shown in Figure 2a, which has several high-intensity peaks located approximately at 29.2° and 35.1°. Upon a closer examination, we can see that there are multiple peaks between 33.97° and 35.08°, which are 34.29°, 34.35° and 34.55°. These three peaks along with the intense peak

at 29.24° match well with the XRD pattern of $CaZnGe_2O_6$ clinopyroxene (PDF Card No.: 00-034-0273). We also noticed extra peaks present in the pattern although the intensity is quite low. These extra peaks can be associated with certain intermediate materials and /or byproducts, such as Zn_2GeO_4 and $Ca_2Ge_7O_{16}$, which have XRD peaks at 30.86°, 33.35°, and 31.52°, 31.82° respectively (PDF Card No.: 04-007- 5691 and PDF Card No.: 00-034-0286).[40, 41] Since the intensities of these impurities are very weak, we can concluded that the majority of product of our solid-state synthesis is the CZGO clinopyroxene.

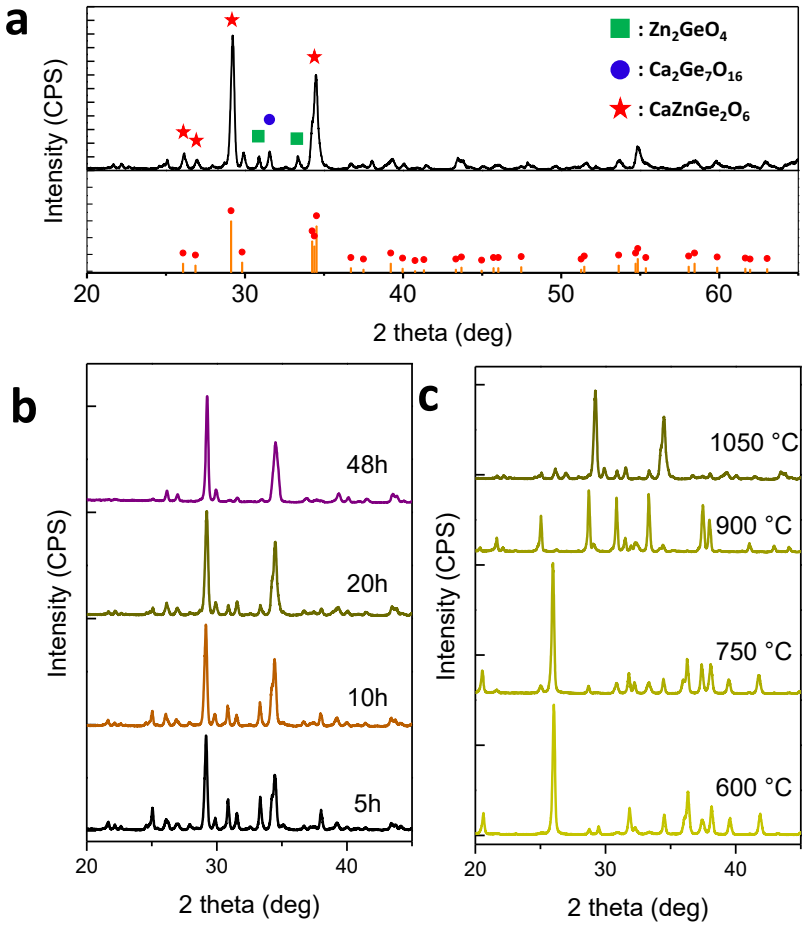

Figure 2. (a) XRD pattern of CZGO: 0.5% Pb and database reference; XRD patterns of CZGO: 0.5% Pb synthesized at 1050 °C for different times (b) and at different temperatures for 20 hours (c).

Solid-state synthesis conditions have a direct impact on the crystal structure and phase purity, which can influence the optical properties of the material. Therefore, it is crucial to thoroughly examine and optimize these

reaction conditions. Here, two series of experiments were carried out to evaluate the impact of reaction time and temperature. For the first set of experiments, we maintained a standard synthesis temperature of 1050 °C, and the reactions were carried out at four different time intervals: 5 hours, 10 hours, 20 hours, and an extended duration of 48 hours. From the XRD data (Figure 2b), intermediates, such as Zn_2GeO_4 at 30.86° and 33.35°, were observed between these major peaks, along with the presence of $Ca_2Ge_7O_{16}$ in the samples (peaks at 31.52° and 31.82°). It was observed that these impurities and intermediate peaks decreased with a longer reaction time, which suggested that the reaction is continuously ongoing until a 20-hour time period. This overall trend suggests that a longer reaction time can yield a purer product, which has cleaner XRD patterns with fewer and weaker intermediates peaks. Notably, the reaction time also exerts an intriguing influence on the photoluminescence color. At shorter reaction times, the CZGO clinopyroxene retains its primary static green fluorescence and red persistent luminescence, as depicted in Figure S2. However, the 20-hour and 48-hour reaction times unveil a captivating dynamic fluorescence effect, which is similar to the phenomenon shown in Figure 1.

To investigate the temperature-dependent effects, a series of CZGO materials was synthesized for a reaction time of 20 hours using various temperatures. Their XRD data are shown in Figure 2c. At both 600 °C and 750 °C, only raw materials are detected, including ZnO, CaO, and GeO_2. For materials synthesized at 900 °C, some intermediates begin to form, such as Zn_2GeO_4 and $Ca_2Ge_7O_{16}$. At 1050 °C, the CZGO samples exhibit the major peaks of CZGO clinopyroxene at 28.94°, 34.29°, 34.35° and 34.55° while the intermediate peaks are of very low intensity. These findings clearly indicate that it is necessary to have the reaction at 1050 °C or above for the CZGO syntheses.

Interestingly, dopant concentration plays an important role in the formation of CZGO. At lower concentrations of lead ions within the clinopyroxene host, intermediates emerge in the product, as elucidated in the XRD data in Figure 3a. However, as the dopant concentration exceeds 3%, the intensity of these intermediate peaks gradually diminishes, resulting in a cleaner XRD pattern. With the increase in dopant concentration, the peak intensity ratio between $Ca_2Ge_7O_{16}$ and CZGO decreases (Figure S3). It seems that the lead dopants acted like a

"catalyst" that can increase the reaction rate for the solid-state synthesis. However, the exact cause of this phenomenon is still unclear and requires further investigation.

Furthermore, the dopant concentration has a significant influence on the optical properties of the synthesized CZGO clinopyroxene, as shown in Figure 3b. All these CZGO tablets give a similar pale white color under ambient lighting. Under UV lamp irradiation, these tablets emit a strong fluorescence. For non-doped CZGO, the fluorescence is green. It remains green fluorescence when the lead dopant is below 1.0%. When the dopant concentration further increases, the fluorescence color changes to yellow, orange, and eventually red. Meanwhile, most of these tablets have a strong PersL (except samples of 0 and 0.1% dopant). The PersL color changes from pinkish red to a solid red for CZGO with high concentrations of lead doping. These sets of CZGO materials with vivid and colorful fluorescence and persistent luminescence are ideal for constructing complex anti-counterfeiting applications.

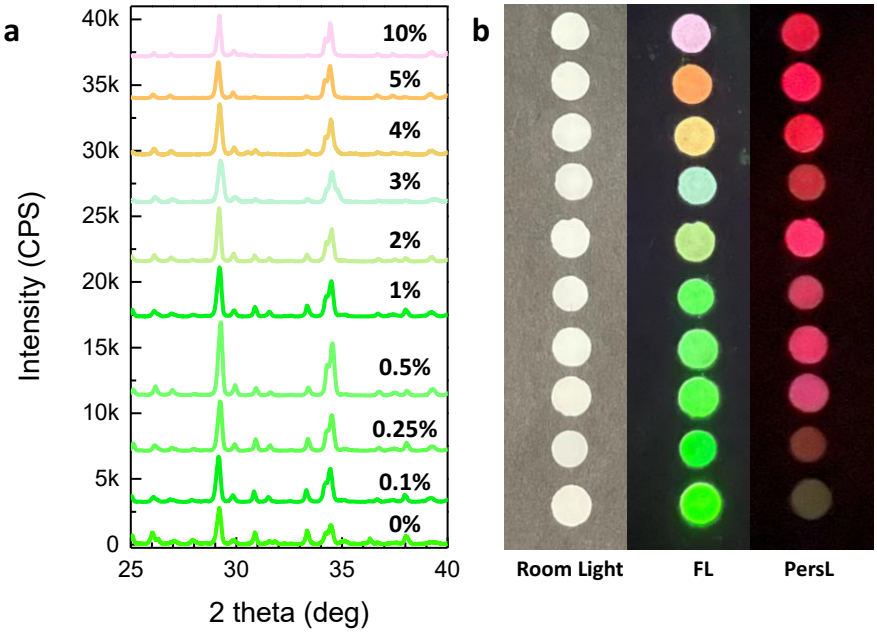

Figure 3. (a) XRD patterns of CZGO doped with different concentrations of Pb^{2+}; (b) Optical images of CZGO tablets with different dopant concentrations.

Among all the different dopant concentrations, we found that the CZGO: 0.25% Pb has the overall best dynamic fluorescence performance. With a careful examination of this sample, we noticed that the phosphor's

natural color changes after exposure to 254 nm UV light, indicating the presence of photochromic properties in this phosphor material. To delve deeper into this phenomenon, we studied reflectance spectroscopy on this phosphor sample, as presented in Figure 4a. The unexposed sample, when compared to the background KBr, shows a very high total reflectance (>98%) between 385 nm to 800 nm. Once the sample was exposed to 254 nm UV light for five minutes, it showed a substantial decrease in absolute reflectance as compared to the unexposed sample, especially from 385 nm to 600 nm. By comparing the reflectance difference between the exposed sample and the unexposed sample, we constructed an absorption curve (Figure S4). This absorption curve showed a broad absorption peak around 380 nm, which indicates the phosphor has a yellowish color. To visually illustrate the photochromic transformation, we compacted the phosphor into a pellet and shielded it with a mask bearing the hollowed symbol of "λ". After exposing the sample to the UV light for five minutes, the sample clearly exhibited a grayish-yellow "λ" symbol on the white pellet, showcasing the photochromic property. It is important to note that this photochromic property is fully reversible, as the sample will slowly change back to white under room temperature and ambient lighting conditions in a period of eight hours.

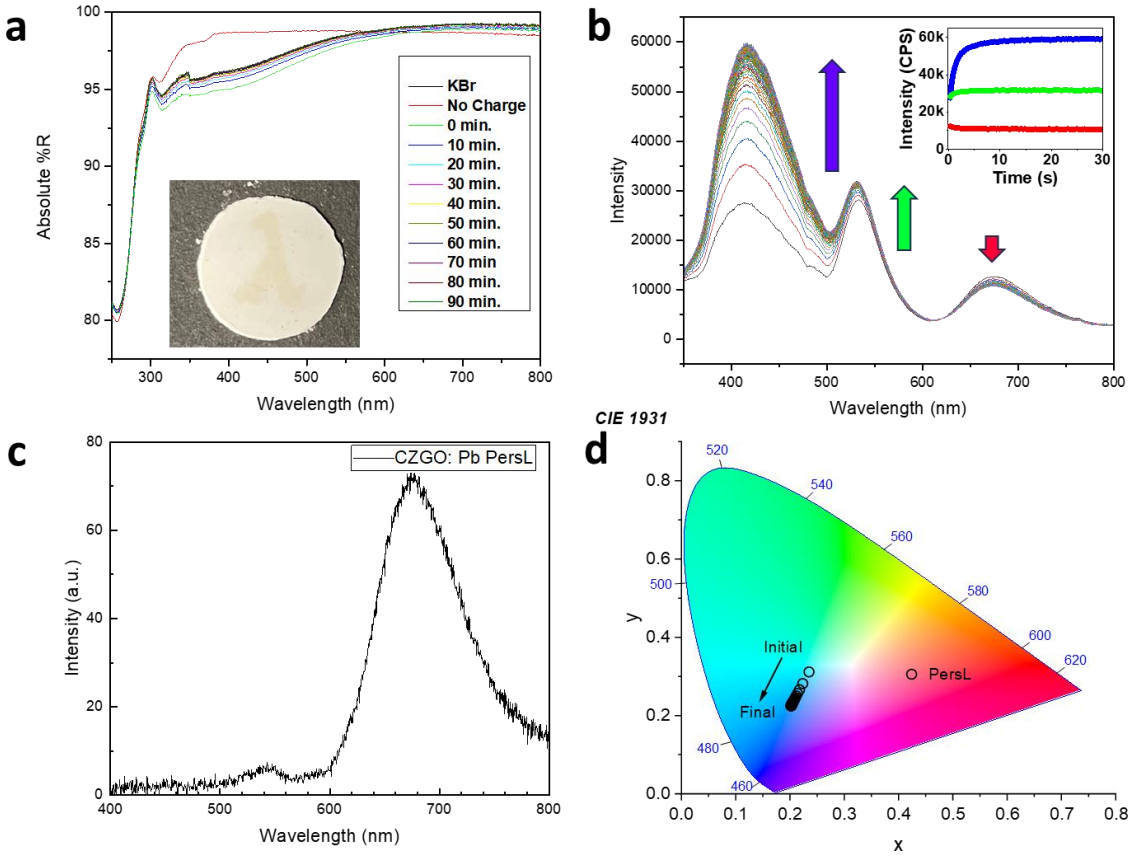

Figure 4: (a) Absolute reflection spectrum of CZGO: 0.25% Pb before and after UV irradiation (insert: optical image of CZGO: 0.25% Pb sample after irradiation with 254 nm UV lamp); (b) Dynamic fluorescence spectrum of CZGO: 0.25% Pb (insert: kinetics study of three emission behavior); (c) Persistent luminescence spectrum of CZGO: 0.25% Pb; (d) CIE plot of initial fluorescence, final fluorescence, and persistent luminescence.

The dynamic fluorescence properties of this material were thoroughly explored and evaluated. As shown in Figure 4b, the phosphor material has three emission peaks under 254 nm UV excitation, 417 nm (blue), 532 nm (green) and 672 nm (red). With a continuous excitation of UV light for 60 s, the intensity of blue peak significantly increases; the green peak has a moderate increase, and the red peak has a minor decrease in intensity. Further analysis revealed the kinetic curve of these three emissions, as shown in the insert. Notably, the blue emission has the highest magnitude of change in its intensity, and it took 15 s to reach an intensity saturation, while the green emission achieves its maximum intensity at around five seconds. The combination of these two

kinetic behaviors results in the dynamic change of the phosphor's fluorescence from green to blue. The entire kinetics process is illustrated in the waterfall plot shown in Figure S5. The change of fluorescence could be reversed when the phosphor material is fully relaxed, typically within 30 min under room temperature and ambient lighting.

Additionally, the phosphor material also demonstrates a broad persistent luminescence emission at 673 nm, which gives this phosphor material a red afterglow (Figure 4c). The CIE plot, shown in Figure 4d, reflects the color of the dynamic fluorescence and the persistent luminescence. The fluorescence color of the phosphor will continuously shift from teal (X: 0.235 Y: 0.312) to light blue (X: 0.202 Y: 0.225) over time, and when the UV irradiation is removed, the persistent luminescence assumes a red color (X: 0.424 Y: 0.306). This rapid blue shift in emission color is very obvious and could be very promising for applications in dynamic anti-counterfeiting.

The unique luminesce properties of CZGO: Pb clinopyroxene can be attributed to its well-defined crystalline structures of the host materials, as well as the perfect fit of the dopant ions in the host matrix. When examining the synthesized undoped CZGO, its XRD patterns match those in the crystallography database, and the crystal structure which is reproduced using a previously published cif file is shown in Figure 5a.[42] It is expected that Pb^{2+} ions would replace the Ca^{2+} ions due to their same coordination number and similar ionic radii.[17] Furthermore, we hypothesized that Pb^{2+} plays a crucial role in the phosphor's photoluminescence properties. Upon investigating the luminescence properties of the undoped CZGO and the CZGO: Pb, we observed only one peak at 532 nm in the emission spectrum while the lead-doped material has three emission peaks (Figure S6). This suggests that the blue (414 nm) and red (672 nm) emissions are originated from the lead dopant center. Consequently, we propose a mechanism to explain the dynamic fluorescence and persistent luminescence properties of CZGO: Pb materials, as depicted in Figure 5b. The band gap of CZGO (4.19 eV) was determined by measuring the UV-visible spectra of a CZGO: Pb dilute suspension (Figure S7) and then calculated according to the known Tauc's method.[43] Under 254 nm UV excitation, the excited electrons will jump to the conduction band.

Some electrons will migrate to the color trap state via nonradiative relaxation. Under UV excitation, the electrons in the color trap state will be able to absorb photons and jump to the conduction band, giving the phosphor a yellowish color in return, thus, contributing to the photochromism properties. With the removal of the UV excitation, the electrons in the color trap will be depleted over time, resulting in the reversal of the photochromism.

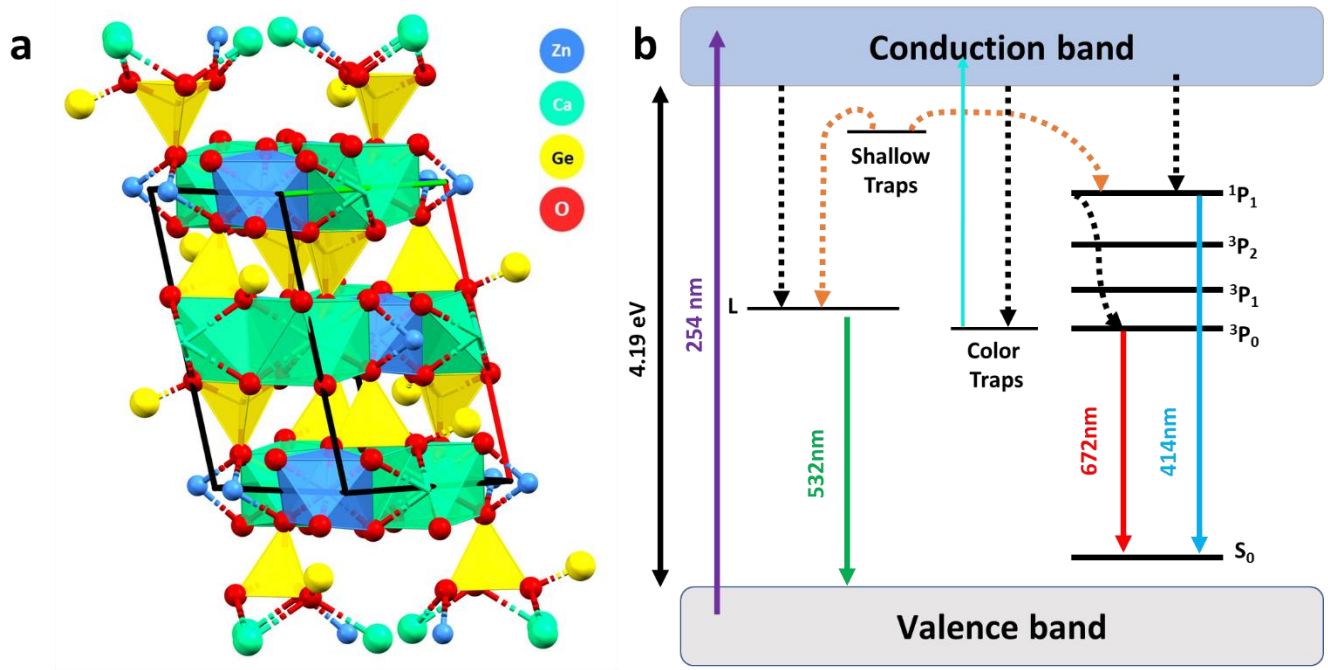

Figure 5. (a) Crystal structure of CZGO (reproduced with permission of the International Union of Crystallography); (b) proposed mechanism of CZGO: 0.25% Pb clinopyroxene.

The remaining electrons in the conduction band will migrate to the states in both the CZGO host and Pb^{2+} dopants. Following this process, the electrons in the matrix's luminescence states will further relax to the valence band and emit 532 nm green emission. The electrons in the Pb^{2+} states will divide into two pathways, the first pathway will lead to relaxation from $^1P_1$ state to S_0, emitting 424 nm blue light. The other electrons will relax to $^3P_0$ before relaxing to S_0, thus emitting the 672 nm red emission. We hypothesize that the electrons initially trapped in the shallow traps may migrate to both the Pb^{2+} and matrix sites. With a closer distance between the two states, the electrons are more likely to migrate to the Pb^{2+} states. With the continuous UV excitation, more

oxygen vacancies are generated, leading to the increase in the number of shallow traps. This process contributes to the gradual increase in blue and green fluorescence intensity. The oxygen vacancies will eventually reach saturation, thus resulting in the saturation of blue emission. However, further studies are required to validate this hypothesis.

Utilizing different CZGO: Pb clinopyroxene materials with manganese-doped zinc germanate phosphors (ZGO), we painted a label of a Christmas tree on black paper, as shown in Figure 6a. Under the room light, the label appears predominantly white and grey, with only some ornaments discernible, while the other ones remain nearly unnoticeable. However, under 254 nm UV excitation (as depicted in Figure 6b), the label transformed into a colorful image featuring a bright green outline, a green Christmas tree, and various ornaments of distinct shapes and colors, including sangria ovals, blue squares, mako triangles, purple diamonds, and a spectra star. The bright outline originates from our previously reported Zn_2GeO_4: Mn, and the green Christmas tree was painted using undoped CZGO. The various colorful fluorescence emissions for the ornaments are associated with different percentages of lead in the CZGO clinopyroxene (Figure S8). Once the UV lamp is turned off, the Christmas tree outline remains visible, though the tree itself becomes barely discernible. All these colorful ornaments now show red emissions with different intensities. These red ornaments will fade over time at different rates (Figure 6c). The square and triangle ornaments will disappear fast, while the circle and the star lose their emission at a much slower rate. This creates dynamic images that can be observed by the naked eyes and captured with a normal camera. When comparing the luminescence intensities, 5% Pb and 10% Pb doped CZGO have noticeably stronger PersL intensity than those with less percentage of dopants (Figure 6d). On the other hand, CZGO: 4% Pb has the longest PersL half-life of 0.55 s, with CZGO: 5% Pb following (Figure 6e). CZGO: 3% Pb has the fastest half-life of 0.26 s, around half of CZGO: 4% Pb. Consequently, the square ornaments (3%) disappear first, followed by the diamond ornaments while the star (4%) and oval ornaments (5%) are still visible after 30 s. With that, we successfully demonstrated the potential of utilizing CZGO clinopyroxenes with various amounts of lead dopants to create multimode colorful labels that have dynamic luminescence properties for anti-counterfeiting.

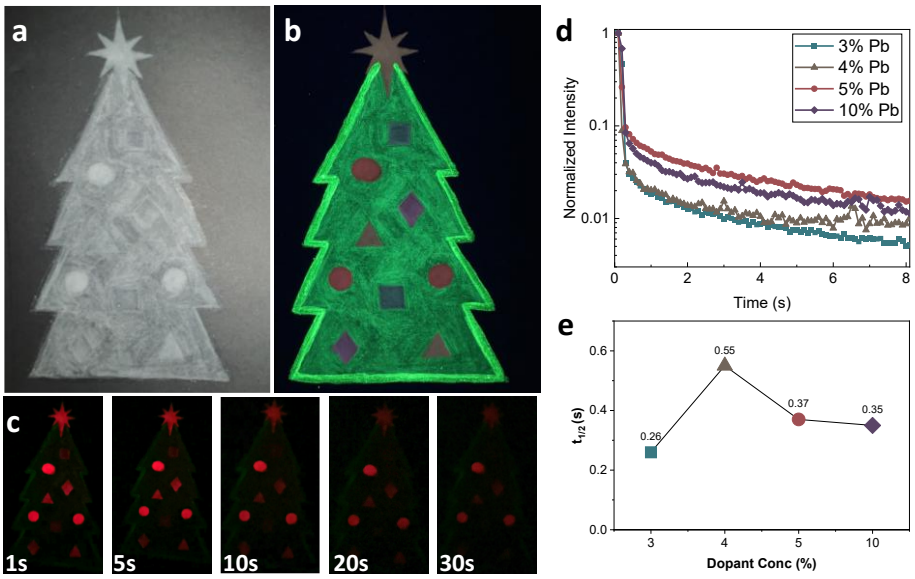

Figure 6. Christmas tree pattern constructed with various germinate materials with (a) room light and (b) 254 nm irradiation; (c) persistent luminescence image of Christmas tree under different time gate; (d) persistent luminescence decay curve of CZGO: Pb; (e) persistent luminescence half-life of CZGO: Pb samples.

CZGO: Pb clinopyroxene could be further applied to construct applications for hidden information storage. To demonstrate this, a PVC card was laser engraved with digital numerical patterns and the trenches were filled with CZGO, CZGO: 0.25% Pb, and regular cornstarch. When viewed under room light, the numbers on the card display as "8888," as depicted in Figure 7a. These numbers appear uniformly due to the similar texture of CZGO, doped CZGO, and cornstarch. With that, no valuable information can be revealed. However, when exposing the PVC card to 254 nm UV light, we can clearly observe a hidden number “8096”. Upon closer examination, we can see some portions of the numbers have different intensities, which can be either neglected when viewed from a distance or further optimized to achieve a better match. Furthermore, a second hidden number, “6735,” will only show up when the UV source is removed, which fades within five seconds. This hidden information is safeguarded with two layers of security, demonstrating the potential application of CZGO clinopyroxene for highly secure hidden information storage.

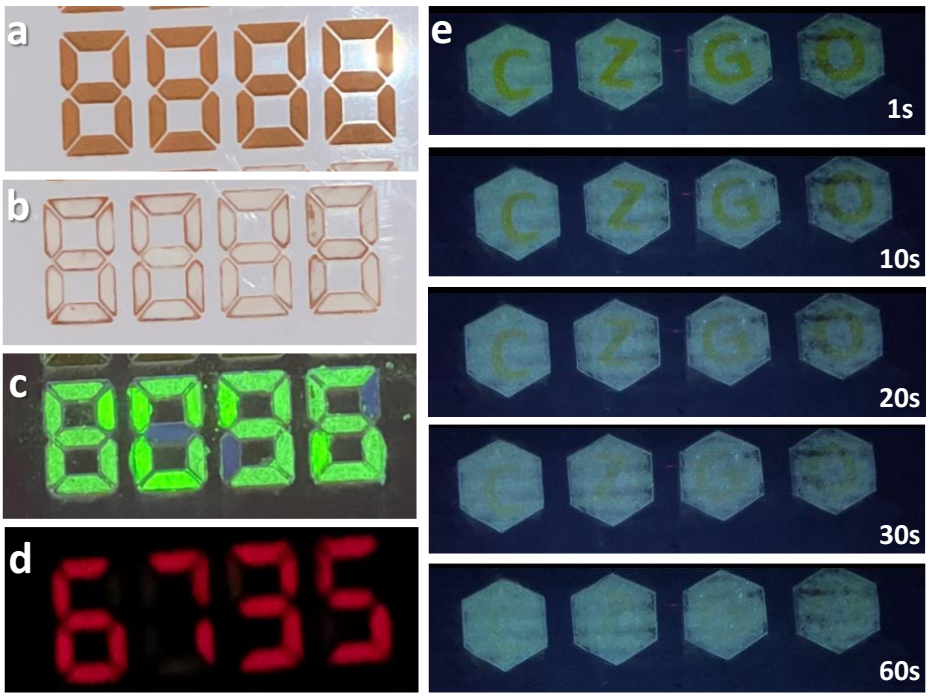

Figure 7. Optical image of (a) laser engraved ID card; encrypted numbers using CZGO: 0.25% Pb phosphor under (b) room light; (c) 254 nm UV light, and (d) removal of 254 nm UV light; (e) optical images of erasable information storage under different time stamps.

Erasable information storage could also be achieved with the phosphor. As shown in Figure 7e, four hexagon patterns were prepared with CZGO: 0.25% Pb. Four letter masks, “C”,“Z”,“G” and “O” were positioned on the hexagon before exciting with 254 nm UV light for 5 min. After five minutes, the masks were then removed, and we recorded the patterns’ changes over time under continuous UV Irradiation. Initially, the hexagon is teal in color, while the letters are yellowish-green. As time passes, the green letters slowly blend into the background as the color changes. This change of fluorescence color is observable both with a camera and the naked eye. Finally, after 60 s, the letters adopted the same color as the background and became completely unnoticeable. Consequently, the encrypted information is no longer recoverable. Furthermore, if the encrypted information is not observed under UV light, the background material will slowly relax back to its initial state, thus erasing the information as well. This application showed that we could utilize the phosphor material for short-term and time-sensitive information storage that is self-erasable over time.

To demonstrate the full potential of CZGO phosphor in anti-counterfeiting applications, we created a highly intricate tyrannosaurus rex (T-Rex) label. As shown in Figure 8a, we observe a detailed T-Rex head under ambient light. When exposed to 254 nm UV excitation, a green T-Rex head with a bright outline becomes visible. As UV irradiation continues, the detailed features of the T-Rex's head undergo a color transformation from green to blue. Only the green outline will appear if we use 385 nm UV to excite the label (Figure S9). Upon removing the UV irradiation, the outline and a purple T-Rex skull are visible while the "meat and skin" portion of the T-Rex are no longer discernible. Notably, the purple skull and the outline will also decay over time. Overall, this T-Rex pattern changes from white to green, then from full green to partial blue, and finally to purple, that fades away. Additionally, the pattern's shape and details also change, from a dinosaur's head to a fossilized skull. In this example, three distinct luminescence properties of the material are demonstrated, along with two unique dynamic changes: dynamic fluorescence from green to blue and the decay of persistent luminescence. The T-rex pattern was exposed under UV for the color change, and the process was repeated several times, even after a storage of six months in a normal condition. The color and intensity of the pattern remained unchanged (Figure S10). Thus, our anti-counterfeiting labels show good cycle stability in practical usage. This work proves the feasibility of creating complex multi-mode security labels using our synthesized CZGO materials, which can be easily decoded and verified using a common UV light source.

Lead-containing materials are, in general, harmful to the human body, especially to young children. For any practical applications, the exposure of lead should be carefully controlled. Fortunately, our designed CZGO material contains only a very modest amount of lead dopant (0.25 %) yet is still able to deliver outstanding dynamic fluorescence performance. Additionally, CZGO material will be blended with a carrier medium, further lowering the lead concentration. Moreover, when we use the CZGO-contained medium as a security label on a driver's license or similar document, the size of the security pattern will be relatively small compared to the overall license. After thorough analysis, we have determined that the final product with a CZGO label will have a lead concentration at a level of 1 ppm, much less than the EPA's 90 ppm limit for commercial paints. In the future, we

might reduce the lead amount even further by adjusting the fabrication process, refining patterns, reducing layer thickness, and utilizing post-production processes such as encapsulation to prevent close contact with the lead-contained paint.

When compared to other luminescence-based materials, CZGO: Pb has the following advantages: Firstly, it is not common for fluorescence materials, especially inorganic phosphors, to have dynamic fluorescence properties. Thus, this type of novel material is an excellent alternative to the conventional luminescence materials. Secondly, compared to organic phosphors, which could have dynamic properties, CZGO: Pb has the advantage of high stability since it has better thermostability, chemoresistance, and photo resistance. Last but not least, CZGO: Pb has photochromic, dynamic fluorescence, and persistent luminescence, which makes it extremely difficult for counterfeiters to reverse engineer. On the other hand, the disadvantages of this material include a limited color range when compared to other phosphor materials. So far, our materials are limited to the blue and green regions of photoluminescence. In the future, we aim to synthesize similar materials with a much broader range of luminescence. Additionally, although CZGO: Pb phosphor shows good performance under short-wavelength UV, it lacks strong emission with long-wavelength excitation, which could also limit the usage of this material in practical applications.

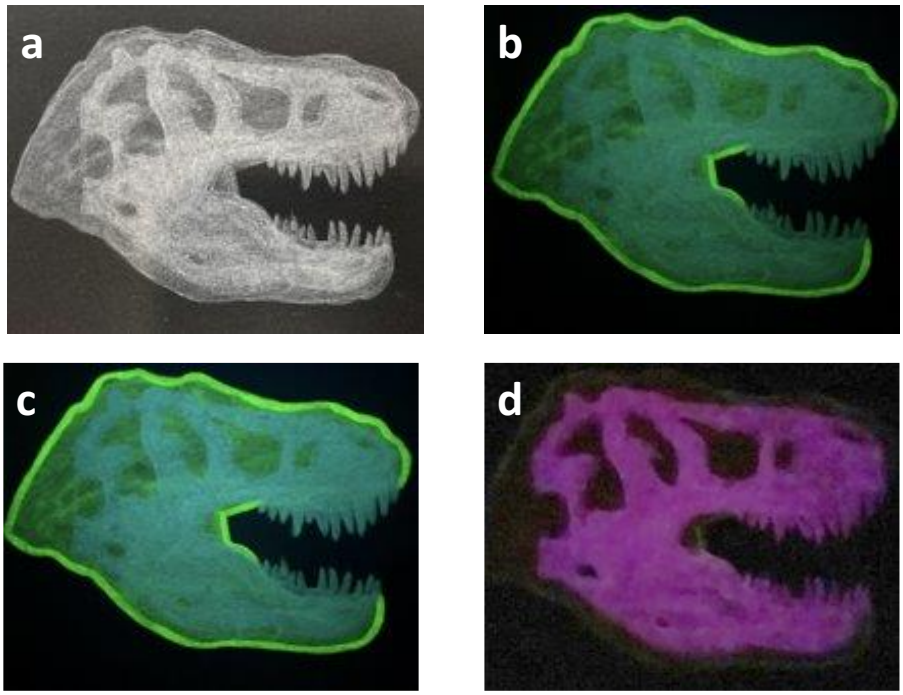

Figure 8. Optical images of T-rex constructed using CZGO and ZGO phosphors under (a) room light; (b) 254 nm UV light, (C) 254 nm UV light after 30 s, and (d) after 254 nm UV light removed.

Conclusion

In conclusion, we have synthesized lead-doped calcium zinc germanate phosphor materials that exhibit unique photochromatic behavior and dynamic fluorescent properties. By varying the dopant concentration, we have synthesized CZGO phosphors with various colors of fluorescence and persistent luminescence emissions. These Pb-doped CZGO phosphors have demonstrated great potential in fabricating anti-counterfeiting labels due to their photochromatic properties, dynamic green-to-blue fluorescence, and the tunable decay of red persistent luminescence. With further optimization, these germanate phosphors will be a key functional material in preparing highly secure anticounterfeiting labels with multilevel encoding and unique optical performance that can be easily visualized for practical applications.

Supporting Information

Optical Images of freshly exposed phosphor materials and phosphor synthesized under different reaction times; impurity peak relationship with dopant concentration plot; calculated UV absorption plot; waterfall plot of dynamic fluorescence; UV absorption of phosphor/ water suspension and calculated Tauc plot; Christmas tree schematic pattern and optical image of T-Rex fluorescence under long wavelength UV.

Author information

Corresponding Author

Chaoyang Jiang - *Department of Chemistry, University of South Dakota, Vermillion, SD 57069, USA*; Email: CY.Jiang@usd.edu

Authors

Zishen Yang - *Department of Chemistry, University of South Dakota, Vermillion, SD 57069*

Levi Spencer - *Department of Chemistry, University of South Dakota, Vermillion, SD 57069*

Huixin Zhang - *Department of Chemistry, University of South Dakota, Vermillion, SD 57069*

Zachary Burmood- *Department of Chemistry, University of South Dakota, Vermillion, SD 57069*

Anjaneyulu Putta - *Department of Chemistry, University of South Dakota, Vermillion, SD 57069*

Author Contributions

The manuscript was written through the contributions of all authors. All authors have given approval to the final version of the manuscript.

Acknowledgments

This work is funded by the South Dakota Governor's Office of Economic Development through the Governor's Research Center for Understanding and Disrupting the Illicit Economy. LS thanks the support from the NSF NRT grant (DGE-1828288).

References:

(1) Ruffato, G.; Rossi, R.; Massari, M.; Mafakheri, E.; Capaldo, P.; Romanato, F. Design, Fabrication and Characterization of Computer Generated Holograms for Anti-Counterfeiting Applications Using Oam Beams as Light Decoders. *Sci. Rep.* **2017**, *7*, 18011.

(2) Chen, C. L.; Yu, Y.; Li, C. G.; Liu, D.; Huang, H.; Liang, C.; Lou, Y.; Han, Y.; Shi, Z.; Feng, S. H. Facile Synthesis of Highly Water-Soluble Lanthanide-Doped t-$LaVO_4$ NPs for Antifake Ink and Latent Fingermark Detection. *Small* **2017**, *13* (48), 1702305.

(3) Zhou, Y. S.; Zhao, G.; Bian, J. M.; Tian, X. L.; Cheng, X. J.; Wang, H.; Chen, H. Y. Multiplexed SERS Barcodes for Anti-Counterfeiting. *ACS App. Mater. Interf.* **2020**, *12* (25), 28532.

(4) Li, D. Y.; Tang, L. H.; Wang, J. J.; Liu, X. J.; Ying, Y. B. Multidimensional SERS Barcodes on Flexible Patterned Plasmonic Metafilm for Anticounterfeiting Applications. *Adv. Opt. Mater.* **2016**, *4* (10), 1475.

(5) Han, S.; Bae, H. J.; Kim, J.; Shin, S.; Choi, S. E.; Lee, S. H.; Kwon, S.; Park, W. Lithographically Encoded Polymer Microtaggant Using High-Capacity and Error-Correctable QR Code for Anti-Counterfeiting of Drugs. *Adv. Mater.* **2012**, *24* (44), 5924.

(6) Sun, Y. J.; Lou, D. Y.; Liu, W.; Zheng, Z. K.; Chen, X. D. SERS Labels for Optical Anticounterfeiting: Structure, Fabrication, and Performance. *Adv. Opt. Mater.* **2023**, 2201549.

(7) Huo, Y. F.; Yang, Z. S.; Wilson, T.; Jiang, C. Y. Recent Progress in SERS-Based Anti-Counterfeit Labels. *Adv. Mater. Interf.* **2022**, *9* (17), 2200201.

(8) Singh, R.; Singh, E.; Nalwa, H. S. Inkjet Printed Nanomaterial Based Flexible Radio Frequency Identification (RFID) Tag Sensors for the Internet of Nano Things. *RSC Adv.* **2017**, *7* (77), 48597.

(9) Dai, X. R.; Wang, K.; Lei, L.; Xu, S. Q.; Cheng, Y.; Wang, Y. S. Pumping-Controlled Multicolor Modulation of Upconversion Emission for Dual-Mode Dynamic Anti-Counterfeiting. *Nanophotonics* **2020**, *9* (6), 1519.

(10) Jiang, X.; Wu, M.; Zhang, L.; Wang, J.; Cui, M.; Wang, J.; Pang, X.; Song, B.; He, Y. Multi-Functional Hydrogels Simultaneously Featuring Strong Fluorescence, Ultralong Phosphorescence, and Excellent Self-Healing Properties and Their Use for Advanced Anti-Counterfeiting. *Anal. Chem.* **2022**, *94* (20), 7264.

(11) Wang, B.; Wang, Z.; Mao, P.; Wang, Y. A Multi-Color Persistent Luminescent Phosphor Beta-$NaYF_4:RE^{3+}$ (RE = Sm, Tb, Dy, Pr) for Dynamic Anti-Counterfeiting. *RSC Adv.* **2022**, *12* (18), 11534.

(12) Xiong, S.; Xiong, Y.; Wang, D.; Pan, Y.; Chen, K.; Zhao, Z.; Wang, D.; Tang, B. Z. Achieving Tunable Organic Afterglow and UV-Irradiation-Responsive Ultralong Room-Temperature Phosphorescence from Pyridine-Substituted Triphenylamine Derivatives. *Adv. Mater.* **2023**, *35* (28), 2301874.

(13) Liu, J. B.; Zhuang, Y. X.; Wang, L.; Zhou, T. L.; Hirosaki, N.; Xie, R. J. Achieving Multicolor Long-Lived Luminescence in Dye-Encapsulated Metal-Organic Frameworks and Its Application to Anticounterfeiting Stamps. *ACS App. Mater. Interf.* **2018**, *10* (2), 1802.

(14) Katumo, N.; Ruiz-Preciado, L. A.; Kumar, V.; Hernandez-Sosa, G.; Richards, B. S.; Howard, I. A. Anticounterfeiting Labels with Smartphone-Readable Dynamic Luminescent Patterns Based on Tailored Persistent Lifetimes in $Gd_2O_2S:Eu^{3+}/Ti^{4+}$. *Adv. Mater. Tech.* **2021**, *6* (7), 2100047.

(15) Yang, Y.; Li, Y.; Chen, Y.; Wang, Z.; He, Z.; He, J.; Zhao, H. Dynamic Anticounterfeiting through Novel Photochromic Spiropyran-Based Switch@Ln-MOF Composites. *ACS App. Mater. Interf.* **2022**, *14* (18), 21330.

(16) Yuan, J.; Christensen, P. R.; Wolf, M. O. Dynamic Anti-Counterfeiting Security Features Using Multicolor Dianthryl Sulfoxides. *Chem. Sci.* **2019**, *10* (43), 10113.

(17) Dong, W.; Wang, W.; Wang, M.; Zhang, J.; Wang, Y. A Dynamic Irradiation-Responsive Material for Advanced Anti-Counterfeiting in Dark and Bright Fields. *J. Mater. Chem. C* **2022**, *10* (11), 4218.

(18) Yang, Y.; Zhao, H.; Li, Y.; Chen, Y.; Wang, Z.; Wu, W.; Hu, L.; Zhu, J. Tuning the Photochromism of Spiropyran in Functionalized Nanoporous Silica Nanoparticles for Dynamic Anticounterfeiting Applications. *ACS Omega* **2023**, *8* (18), 16459.

(19) He, Z.; Li, Y.; Wu, H.; Yang, Y.; Chen, Y.; Zhu, J.; Li, Q.; Jiang, G. Novel Stimuli-Responsive Spiropyran-Based Switch@HOFs Materials Enable Dynamic Anticounterfeiting. *ACS App. Mater. Interf.* **2022**, *14* (42), 48133.

(20) Fu, S. C.; Liu, Y. C.; Dong, L.; Lu, Z. F.; Hu, W. L.; Xie, M. G. Photo-Dynamics of Polarization Holographic Recording in Spirooxazine-Doped Polymer Films. *Mater. Lett.* **2005**, *59* (11), 1449.

(21) Klajn, R. Spiropyran-Based Dynamic Materials. *Chem. Soc. Rev.* **2014**, *43* (1), 148.

(22) Cui, Z.; Deng, G. W.; Wang, O. U.; Luo, X. L.; Li, Z. H.; Yang, M.; Cheng, S. H.; Liu, X. Y. Controllable Synthesis and Luminescence Properties of Zn_2GeO_4 : Mn^{2+} Nanorod Phosphors. *ChemistrySelect* **2021**, *6* (39), 10554.

(23) Lan, N. M. C. H. P.; Thang, C. X.; Kien, N. D. T.; Tung, N. V. Hydrothermal Synthesis of Zn_2GeO_4 and Mn^{2+} Doped Zn_2GeO_4 (Zgo) Nanoparticles with Controlled Luminescent Properties. *Mater. Trans.* **2022**, *63* (2), 197.

(24) The Materials, P. Materials Data on Zn_2GeO_4 by Materials Project. United States, 2020.

(25) Liu, P.; Ru, Q.; Zheng, P.; Shi, Z.; Liu, Y.; Su, C.; Hou, X.; Su, S.; Chi-Chung Ling, F. One-Step Synthesis of Zn_2GeO_4/CNT-O Hybrid with Superior Cycle Stability for Supercapacitor Electrodes. *Chem. Eng. J.* **2019**, *374*, 29.

(26) Calderón-Olvera, R. M.; Arroyo, E.; Jankelow, A. M.; Bashir, R.; Valera, E.; Ocaña, M.; Becerro, A. I. Persistent Luminescence $Zn_2GeO_4:Mn^{2+}$ Nanoparticles Functionalized with Polyacrylic Acid: One-Pot Synthesis and Biosensing Applications. *ACS App. Mater. Interf.* **2023**, *15* (17), 20613.

(27) Gong, J.-H.; Chen, L.-J.; Zhao, X.; Yan, X.-P. Persistent Production of Reactive Oxygen Species with Zn_2GeO_4:Cu Nanorod-Loaded Microneedles for Methicillin-Resistant Staphylococcus Aureus Infectious Wound Healing. *ACS App. Mater. Interf.* **2022**, *14* (15), 17142.

(28) Chen, X.; Ran, X.; Lu, Y.; Feng, C. Synthesis and Electrochemical Properties of Zinc Germanate Nanowires as Novel Anode Material for Lithium-Ion Battery. *Ionics* **2021**, *27* (10), 4177.

(29) Bender, J. P.; Wager, J. F.; Kissick, J.; Clark, B. L.; Keszler, D. A. Zn_2GeO_4:Mn Alternating-Current Thin-Film Electroluminescent Devices. *J. Lumin.* **2002**, *99* (4), 311.

(30) Gao, D. L.; Ma, K. W.; Wang, P.; Zhang, X. Y.; Pang, Q.; Xin, H.; Zhang, Z. H.; Jiao, H. Tuning Multicolour Emission of Zn_2GeO_4:Mn Phosphors by Li^+ Doping for Information Encryption and Anti-Counterfeiting Applications. *Dalton Trans.* **2022**, *51* (2), 553.

(31) Yang, Z. S.; Spencer, L. D.; Patocka, D. R.; Putta, A.; Schnetzer, E. E.; Kellar, J.; Jiang, C. Y. Manganese-Doped Zinc Germanate Phosphors with Vivid Luminescent Properties for Anti-Counterfeit Applications. *Opt. Mater.* **2023**, *142*, 114036.

(32) Gao, D. L.; Gao, F.; Kuang, Q. Q.; Zhang, X. Y.; Zhang, Z. H.; Pan, Y.; Chai, R. P.; Jiao, H. Zinc Germanate Nanophosphors with Persistent Luminescence for Multi-Mode Imaging of Latent Fingerprints. *ACS App. Nano Matter.* **2022**, *5* (7), 9929.

(33) Ye, K.; Yang, X.; Xiao, S. Improving Red Afterglow Properties of $CaZnGe_2O_6$: Mn^{2+} by Co-Doping Bi^{3+}. *Optik* **2021**, *246*, 167799.

(34) Woo, B. K.; Luo, Z.; Li, Y.; Singh, S. P.; Joly, A. G.; Hossu, M.; Liu, Z.; Chen, W. Luminescence Enhancement of $CaZnGe_2O_6$:Tb^{3+} Afterglow Phosphors Synthesized Using ZnO Nanopowders. *Opt. Mater.* **2011**, *33* (8), 1283.

(35) Kang, R.; Nie, J.; Dou, X.; Zhang, S.; Ju, G.; Chen, L.; Hu, Y.; Li, Y. Tunable NIR Long Persistent Luminescence and Discovery of Trap-Distribution-Dependent Excitation Enhancement in Transition Metal Doped Weak-Crystal-Field $CaZnGe_2O_6$. *J. Alloys Compd.* **2018**, *735*, 692.

(36) Che, G.; Liu, C.; Wang, Q.; Xu, Z. White-Light-Emission Afterglow Phosphor $CaZnGe_2O_6$:Dy^{3+}. *Chem. Lett.* **2008**, *37* (2), 136.

(37) Lin, M.; Gao, Z.; Xu, C.; Yuan, Y.; Tang, Y.; Liu, T.; Sun, L. Enhanced and Broadened NIR Emission of $CaZnGe_2O_6$:Cr^{3+} by Yb^{3+} Codoping for NIR Applications. *ACS App. Opt. Mater.* **2023**, *1* (3), 724.

(38) Wang, M.; Wu, H.; Dong, W.; Lian, J.; Wang, W.; Zhou, J.; Zhang, J. Advanced Luminescence Anticounterfeiting Based on Dynamic Photoluminescence and Non-Pre-Irradiation Mechanoluminescence. *Inorg. Chem.* **2022**, *61* (6), 2911.

(39) Dou, X.; Xiang, H.; Wei, P.; Zhang, S.; Ju, G.; Meng, Z.; Chen, L.; Hu, Y.; Li, Y. A Novel Phosphor $CaZnGe_2O_6$:Bi^{3+} with Persistent Luminescence and Photo-Stimulated Luminescence. *Mater. Res. Bull.* **2018**, *105*, 226.

(40) Hang, C.; Simonov, M. A.; Belov, N. V. Crystal Structures of Willemite $Zn_2[SiO_4]$ and Its Germanium Analog $Zn_2[GeO_4]$. *Soviet Physics Crystallography, Ussr* **1970**, *15* (3), 387.

(41) Nevskii, N. N.; Iliukhin, V. V.; Ivanova, L. I.; Belov, N. V. Crystal-Structure of Calcium Germanate, $Ca_2Ge_2[GeO_4][Ge_4O_{12}]$. *Doklady Akademii Nauk Sssr* **1979**, *245* (1), 110.

(42) Redhammer, G. J.; Roth, G. A Comparison of the Clinopyroxene Compounds $CaZnSi_2O_6$ and $CaZnGe_2O_6$. *Acta Crystallogr C* **2005**, *61* (Pt 2), i20. doi.org/10.1107/S0108270104033153

(43) Tauc, J. Optical Properties and Electronic Structure of Amorphous Ge and Si. *Mater. Res. Bull.* **1968**, *3* (1), 37.

TOC